Electromagnetic response of a thin type-II superconducting cylindrical shell

Antonio Pérez-González*
Departamento de Física del Instituto de Ciencias, Universidad Autónoma de Puebla, Apartado Postal J-48, Puebla, Puebla 72570, México

John R. Clem
Ames Laboratory and Department of Physics, Iowa State University, Ames, Iowa 50011
(Received 20 July 1990)

The general critical-state model, which includes the effects of both flux-line cutting and flux pinning, is used for calculating the response of a type-II superconducting cylindrical shell subjected to applied magnetic fields that change in both magnitude and orientation. Analytic expressions for the ac losses are obtained for the case that the applied field has a small-amplitude oscillating component. For the regime of partial penetration of the changing **B** field, the ac-loss expression reduces, for large cylinder radius, to that in slab geometry. When full penetration occurs, the ac-loss expressions depend upon the cylinder outer radius.

I. INTRODUCTION

In a recent series of papers,[1-5] we have stated that, in order to understand the surprising experimental results observed[6-20] in type-II superconductors subjected to parallel magnetic fields that change in both magnitude and direction, flux-line-cutting effects must be included in the theory of static and dynamic magnetic behavior of these materials. The resulting macroscopic theory takes the form of a general critical-state model,[1-4] which includes not only the effects of flux pinning,[21-23] but also the effects of flux-line cutting.[23,24] In this paper, we calculate, using the general critical-state theory, the response of a thin type-II superconducting cylindrical shell when it is subjected to external time-varying magnetic fields.

In Sec. II we develop the general critical-state theory in cylindrical geometry. In Sec. III we specialize the model for the case of a very thin cylindrical shell and show how the basic equations of Sec. II reduce, under proper conditions, to those of slab geometry. We solve these equations and calculate the behavior of the magnetic and electric fields inside the superconducting shell. Section IV focuses on ac losses in the case of an oscillating externally applied magnetic field. Two cases are considered depending upon the degree of penetration in the shell of the changing **B** field. We find for the case of partial penetration i.e., that for which the **B** field in the hole remains unchanged, that the ac losses are the same as those in slab geometry.[4] When complete penetration is achieved, however, the **B** field in the hole changes when the external field changes. This is reflected in an ac-loss expression that depends, to leading order, on the shell's outer radius; this expression does not reduce to that in slab geometry.[4]

II. THE GENERAL CRITICAL-STATE MODEL IN CYLINDRICAL GEOMETRY

Consider a high-κ irreversible type-II superconducting infinite cylinder of radius R. Applied to it is a longitudinal magnetic field $H_z(t)$ and an azimuthal magnetic field $H_\phi = I_z/2\pi R$, where I_z is a current in the z direction along the cylinder axis. We assume that, to good approximation, $\mathbf{B}=\mu_0\mathbf{H}$ inside the sample, and we neglect any surface barriers against vortex entry or exit. We further assume that the magnetic induction **B** inside the cylinder depends only upon the coordinate r and time t, i.e.,

$$\mathbf{B}(r,t)=B(r,t)\hat{\boldsymbol{\alpha}}(r,t) ,$$

where

$$B(r,t)=|\mathbf{B}(r,t)| ;$$

$\hat{\boldsymbol{\alpha}}(r,t)$ is a unit vector locally parallel to **B** (see Fig. 1),

$$\hat{\boldsymbol{\alpha}}(r,t)=\hat{\boldsymbol{\phi}}(r)\sin\alpha(r,t)+\hat{\mathbf{z}}\cos\alpha(r,t) , \tag{1}$$

and $\alpha(r,t)$ is the angle between the z axis and the **B** field.

Writing the current density **J** and the electric field **E** in terms of their components parallel and perpendicular to the local **B**, i.e., $\mathbf{J}=J_\parallel\hat{\alpha}+J_\perp\hat{\beta}$ and $\mathbf{E}=E_\parallel\hat{\alpha}+E_\perp\hat{\beta}$, where

$$\hat{\boldsymbol{\beta}}(r,t)=\hat{\boldsymbol{\alpha}}(r,t)\times\hat{\mathbf{r}}$$
$$=\hat{\boldsymbol{\phi}}(r)\cos\alpha(r,t)-\hat{\mathbf{z}}\sin\alpha(r,t) , \tag{2}$$

we obtain, from Ampère's and Faraday's laws,

$$J_\parallel=\mu_0^{-1}B\left[\frac{\partial\alpha}{\partial r}+\frac{\sin\alpha\cos\alpha}{r}\right] , \tag{3}$$

$$J_\perp=-\mu_0^{-1}\left[\frac{\partial B}{\partial r}+B\frac{\sin^2\alpha}{r}\right] , \tag{4}$$

and

$$\frac{\partial E_\parallel}{\partial r}=B\frac{\partial\alpha}{\partial t}+E_\perp\frac{\partial\alpha}{\partial r}-E_\phi\frac{\sin\alpha}{r} , \tag{5}$$

$$\frac{\partial E_\perp}{\partial r}=-\frac{\partial B}{\partial t}-E_\parallel\frac{\partial\alpha}{\partial r}-E_\phi\frac{\cos\alpha}{r} , \tag{6}$$

where $E_\phi=E_\parallel\sin\alpha+E_\perp\cos\alpha$.

The combination of Eqs. (3) and (6) yields

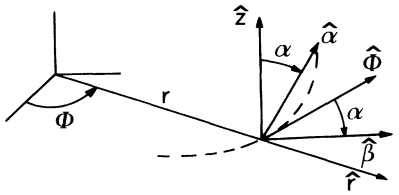

FIG. 1. Sketch of the cylindrical geometry used throughout the paper. $\hat{\alpha}$ is the direction of the **B** field and $\hat{\beta}=\hat{\alpha}\times\hat{\mathbf{r}}$ is perpendicular to $\hat{\mathbf{B}}$, both $\hat{\alpha}$ and $\hat{\beta}$ lie on the ϕ-z plane.

$$\frac{\partial B}{\partial t}+\nabla\cdot\mathbf{j}_B=-\frac{\mu_0 J_\parallel E_\parallel}{B}+\frac{E_\perp\sin^2\alpha}{r}\ , \tag{7}$$

where $\mathbf{j}_B=\hat{\mathbf{r}}j_{Br}=\hat{\mathbf{r}}Bv_r=\hat{\mathbf{r}}E_\perp$ is the B-current density and v_r is the radial component of the velocity of the vortices. Equation (7) can be thought of as an equation of continuity for B. In slab geometry,[2] where $r\to\infty$, this equation reduces to

$$\frac{\partial B}{\partial t}+\nabla\cdot\mathbf{j}_B=-\frac{\mu_0 J_\parallel E_\parallel}{B}\ , \tag{8}$$

which states that a region of space in which flux-line cutting occurs ($J_\parallel E_\parallel>0$) serves as a sink for B; in other words, flux-line cutting consumes B.

In cylindrical geometry there is an additional term present. Here B is not conserved even when $E_\parallel=0$, as can be seen in ordinary flux flow in a wire. In steady state, when $\nabla\times\mathbf{E}=0$, $E_\phi=0$ and $E_z=E_0=$const independent of time. In this case we know that $\mathbf{B}=B_\phi(r)\hat{\boldsymbol{\phi}}(r)$, such that $\hat{\alpha}=\hat{\boldsymbol{\phi}}$, $\hat{\beta}=-\hat{\mathbf{z}}$, $\alpha=\pi/2$, and the **E** field is perpendicular to the local **B** field, i.e., $E_\parallel=0$, $E_\perp=-E_0$. From Eq. (7) we obtain

$$\nabla\cdot\mathbf{j}_B=\frac{E_\perp}{r}=-\frac{E_0}{r}\ , \tag{9}$$

which states that B is being destroyed as a consequence of flux flow. This occurs as vortices shrink in length as they come closer to the axis of the wire.

In nonsteady flux flow, in the absence of a longitudinal field, we still have $\mathbf{B}=B_\phi(r)\hat{\boldsymbol{\phi}}(r)$ and $E_\phi=0$ with $E_\parallel=0$ and $E_\perp=E_z(r,t)$, and from Eq. (7) we get

$$\frac{\partial B}{\partial t}+\nabla\cdot\mathbf{j}_B=\frac{E_\perp}{r}\ , \tag{10}$$

which states again that B is not conserved.

The general critical-state model states that, for slow variations of the magnetic field such that eddy currents are negligible, metastable distributions of B are such that the magnitude of $J_\perp$ is always smaller than the transverse critical-current density at the threshold for depinning in the vortex array

$$|J_\perp|\le J_{c\perp}(B)\ . \tag{11}$$

Similarly, metastable distributions of α are such that the magnitude of $J_\parallel$ is always smaller than the longitudinal critical-current density at the threshold for the onset of flux-line cutting in the vortex array

$$|J_\parallel|\le J_{c\parallel}(B)\ . \tag{12}$$

We assume, in analogy to the usual critical-state model,[21,22] that the electric field behaves as

$$E_\perp=\begin{cases}\rho_\perp[J_\perp-J_{c\perp}(B)]\ , & J_\perp>J_{c\perp}\ ,\\ \rho_\perp[J_\perp+J_{c\perp}(B)]\ , & J_\perp<-J_{c\perp}\ ,\\ 0\ , & |J_\perp|\le J_{c\perp}\ ,\end{cases} \tag{13}$$

and

$$E_\parallel=\begin{cases}\rho_\parallel[J_\parallel-J_{c\parallel}(B)]\ , & J_\parallel>J_{c\parallel}\ ,\\ \rho_\parallel[J_\parallel+J_{c\parallel}(B)]\ , & J_\parallel<-J_{c\parallel}\ ,\\ 0\ , & |J_\parallel|\le J_{c\parallel}\ ,\end{cases} \tag{14}$$

where $\rho_\perp$ and $\rho_\parallel$ are the effective flux-flow and flux-cutting resistivities of the material. Because we assume here that $|E_\perp|\ll\rho_\perp J_{c\perp}$ and $|E_\parallel|\ll\rho_\parallel J_{c\parallel}$, the distributions of **B** computed throughout this paper are independent of $\rho_\perp$ and $\rho_\parallel$.

III. A VERY THIN CYLINDRICAL SHELL

In this section we consider the case of a very thin noncurrent-carrying type-II superconducting cylindrical shell (see Fig. 2) subjected to a constant azimuthal magnetic field at its inner and outer surfaces and a linearly increasing or decreasing applied longitudinal field at its outer surface. The azimuthal fields are $H_\phi(R_i)=I_w/2\pi R_i$ and $H_\phi(R_o)=I_w/2\pi R_o$, and the outer longitudinal field is $H_z(R_o)=H_a$, where R_i and R_o are the inner and outer radii, respectively, and I_w is the current in the z direction along a wire on the cylindrical axis.

We define $W=R_o-R_i$ and $R=(R_o+R_i)/2$, and as-

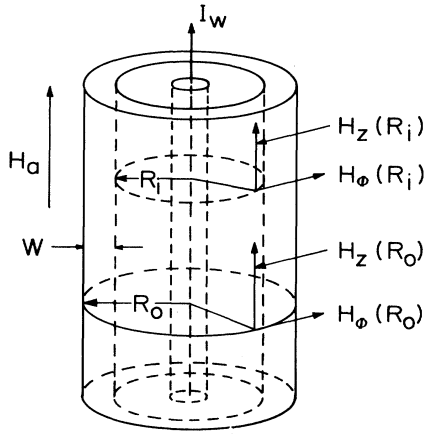

FIG. 2. Sketch of the cylindrical shell considered in Sec. III. The shell thickness W is greatly exaggerated.

sume $W \ll R$. This case corresponds to that of slab geometry if, in addition to the above assumption, we can neglect the line-tension terms, those proportional to $1/r \cong 1/R$, in the basic equations. The second terms on the right-hand sides of Eqs. (3) and (4) become negligibly small by comparison with the first terms when

$$k_{c\parallel} = \mu_0 J_{c\parallel}/B(r) \gg 1/R$$

and (15)

$$\mu_0 J_{c\perp}/B(r) \gg 1/R \ .$$

For simplicity we take $k_{c\parallel}$ and $J_{c\perp}$ to be constants independent of r.

Great care must be taken in considering the boundary conditions in order to avoid inconsistencies like those in Ref. 25. As mentioned in Ref. 26, the results obtained from solving the general critical-state model in slab geometry also apply to a thin-walled cylindrical shell, provided it has a slit along its length, such that the longitudinal fields at both surfaces are the same. We are not considering this case.

For the closed infinite cylindrical shell, the boundary conditions are

$$B_\phi(R_i) = \mu_0 I_w/2\pi R_i \ , \quad B_\phi(R_o) = \mu_0 I_w/2\pi R_o \ , \tag{16}$$

and

$$B_z(R_o,t) = B_a(t) = \dot{B}_a t \ . \tag{17}$$

The condition on $B_z(R_i)$ must be calculated from Faraday's law using the general critical-state model taking into consideration that changes in the longitudinal magnetic field on the inner surface occur through leaking from the outer surface.

We will assume that $W \ll R$ such that we do not need to make a distinction between $B_\phi(R_i)$ and $B_\phi(R_o)$, we thus assume that a field

$$B_\phi(R) = \mu_0 I_w/2\pi R \tag{18}$$

is applied in the azimuthal direction on both surfaces.

The magnetic-field magnitude and angle on the outer and inner surfaces are given by

$$B(R_o,t) = [B_a^2(t) + B_\phi^2(R)]^{1/2} \ , \tag{19a}$$

$$\alpha(R_o,t) = \arctan[B_\phi(R)/B_a(t)] \ , \tag{19b}$$

and

$$B(R_i,t) = [B_i^2(t) + B_\phi^2(R)]^{1/2} \ , \tag{20a}$$

$$\alpha(R_i,t) = \arctan[B_\phi(R)/B_i(t)] \ , \tag{20b}$$

respectively, where $B_i(t) = B_z(R_i,t)$ is the longitudinal component of $B(R_i,t)$.

Consider $E_\perp < 0$ over the wall thickness, i.e., the case in which the entire shell is above threshold for depinning, $J_\perp \cong -J_{c\perp}$ and $dB/dr = \mu_0 J_{c\perp}$, such that

$$B(R_i) = B(R_o) - \mu_0 J_{c\perp} W \ , \tag{21}$$

this determines $B_i(t)$ and $\alpha(R_i,t)$. Keeping terms to first order in $\mu_0 J_{c\perp} W/B$, we obtain

$$B_i(t) = B_a(t) - \frac{[B_a^2(t) + B_\phi^2(R)]^{1/2}}{B_a(t)} \mu_0 J_{c\perp} W \tag{22}$$

and

$$\alpha(R_i,t) = \alpha(R_o,t) + \frac{\mu_0 J_{c\perp} W}{B(R_o)} \tan[\alpha(R_o,t)] \ . \tag{23}$$

From Faraday's law,

$$2\pi R_o E_\phi(R_o,t) \cong -\pi R^2 \dot{B}_i - 2\pi R \int_{R_i}^{R_o} dr \, \dot{B}_z(r,t)$$

because the integral term is of order $2\pi R W \dot{B}_i$, and $\pi R^2 \gg 2\pi R W$, $E_\phi(r,t)$ is dominated by the flux-in-the-hole term and we obtain, for $R_i \le r \le R_o$,

$$E_\phi(r,t) = -\tfrac{1}{2} R \dot{B}_i \ . \tag{24}$$

Assuming that, in the outer region of the superconducting shell, $E_\parallel = 0$, the azimuthal component of the E field is given by

$$E_\phi(r,t) = E_\perp(r,t)\cos\alpha(r,t) \ .$$

Since $\alpha(r,t) \cong \alpha(R,t)$, the radial component of the velocity of the vortices is

$$v_r = \frac{E_\perp}{B} = -\frac{1}{2} \frac{R\dot{B}_i}{B(r,t)\cos\alpha(R_o,t)} \ , \tag{25}$$

but $B(r,t) \cong B(R_o,t)$,

$$B(R_o,t)\cos\alpha(R_o,t) = B_a$$

and to lowest order, $\dot{B}_i = \dot{B}_a$, then $v_r = -R\dot{B}_a/2B_a$, and the time required for a given vortex to move from the outer surface to the inner one is

$$\Delta t = W/v_r = 2B_a W/R\dot{B}_a \ .$$

By the time the vortex has migrated from R_o to R_i, the angle at the outer surface $\alpha(R_o,t)$ has changed by an amount

$$\Delta\alpha_s = \dot{\alpha}(R_o,t)\Delta t = -(W/R)\sin 2\alpha(R_o,t) \ , \tag{26}$$

such that the gradient of α is of order

$$\frac{d\alpha}{dr} \cong \frac{\Delta\alpha_s}{W} = -\frac{\sin 2\alpha(R_o,t)}{R} \ . \tag{27}$$

This is a negligibly small term by comparison with $k_{c\parallel} = \mu_0 J_{c\parallel}/B$, i.e., on the scale of $k_{c\parallel}$ the gradient of α is zero. Thus, the $\alpha(r,t)$ versus r profiles are essentially flat, except for the complication that we cannot have $\alpha(R_i,t) = \alpha(R_o,t)$ because of Eq. (23). That is, vortices arriving to the inner surface would have the wrong angle to match with $\alpha(R_i,t)$. Thus, close to the inner surface there must be a cutting and transport (CT) region over which $\alpha(r,t)$ changes from the value given by Eq. (23) to $\alpha(R_o,t)$ [see Fig. 3(a)[. In the CT region we have $d\alpha/dr = -k_{c\parallel}$, $J_\parallel = -J_{c\parallel}$ and $E_\parallel < 0$. The boundary R_c between the CT zone and the transport (T) zone is defined by

$$\frac{W_c}{W} = \frac{J_{c\perp}}{J_{c\parallel}} \frac{B_\phi(R)}{B_a} = \frac{\tan\alpha(R_o,t)}{\tan\gamma_c} \ , \tag{28}$$

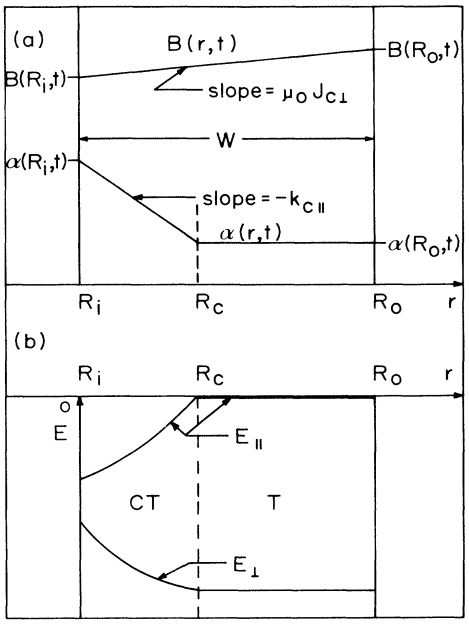

FIG. 3. (a) **B** and (b) **E** behavior inside the cylindrical shell for the flux-pinning dominated regime. There must exist a CT zone close to the inner surface in order to satisfy the boundary conditions on that surface as discussed in Sec. III.

where $W_c = R_c - R_i$,

$$\tan\alpha(R_o,t) = B_\phi(R)/B_a \ ,$$

and $\tan\gamma_c = J_{c\parallel}/J_{c\perp}$. Note that $W_c < W$ when $B_a > B_\phi(R)J_{c\perp}/J_{c\parallel}$.

Neglecting the line tension terms in Eqs. (5) and (6), and because $|Bd\alpha/dt| \ll R\dot{B}_a k_{c\parallel}$, and $|dB/dt| \ll R\dot{B}_a k_{c\parallel}$, we obtain, for $R_i \le r \le R_c$,

$$\frac{dE_\parallel}{dr} = -k_{c\parallel}E_\perp \tag{29}$$

and

$$\frac{dE_\perp}{dr} = k_{c\parallel}E_\parallel \ , \tag{30}$$

from which we get [see Fig. 3(b)]

$$E_\parallel(r,t) = \frac{-E_\phi}{\cos\alpha(R_o,t)}\sin k_{c\parallel}(r-R_c) \ , \tag{31}$$

$$E_\perp(r,t) = \frac{E_\phi}{\cos\alpha(R_o,t)}\cos k_{c\parallel}(r-R_c) \ , \tag{32}$$

where E_ϕ is given by Eq. (24). $E_z(t)$ is independent of r in both the CT and T regions and is given by

$$E_z(t) = -E_\phi\tan\alpha(R_o,t) \ . \tag{33}$$

Depending upon the relation between $J_{c\parallel}$ and $J_{c\perp}$, $\tan\alpha(R_o,t)$ can be larger than, equal to, or smaller than $\tan\gamma_c$. The case discussed above corresponds to the regime

$$\tan\alpha(R_o,t) < \tan\gamma_c \ ,$$

which is flux-pinning dominated in the sense that the entire shell is above threshold for depinning. When

$$\tan\alpha(R_o,t) = \tan\gamma_c \ ,$$

$W_c = W$, and the critical-angle gradient fills up the shell thickness, producing a single CT zone over the entire wall.

We next consider the case for which $B_a < B_\phi(R)J_{c\perp}/J_{c\parallel}$ or

$$\tan\alpha(R_o,t) > \tan\gamma_c \ .$$

In this regime, the behavior must be dominated by flux-line cutting, and the critical-angle gradient determines $B(R_i)$. Consider $E_\parallel < 0$ over the wall thickness, i.e., the case in which the entire shell is above threshold for flux-line cutting, $J_\parallel = -J_{c\parallel}$, and $d\alpha/dr = -k_{c\parallel}$, such that

$$\alpha(R_i) = \alpha(R_o) + k_{c\parallel}W \ . \tag{34}$$

Keeping terms to first order in $k_{c\parallel}W$, we obtain

$$B(R_i) = B(R_o)[1 - k_{c\parallel}W\cot\alpha(R_o)] \ . \tag{35}$$

Note that since $\tan\gamma_c/\tan\alpha(R_o) < 1$,

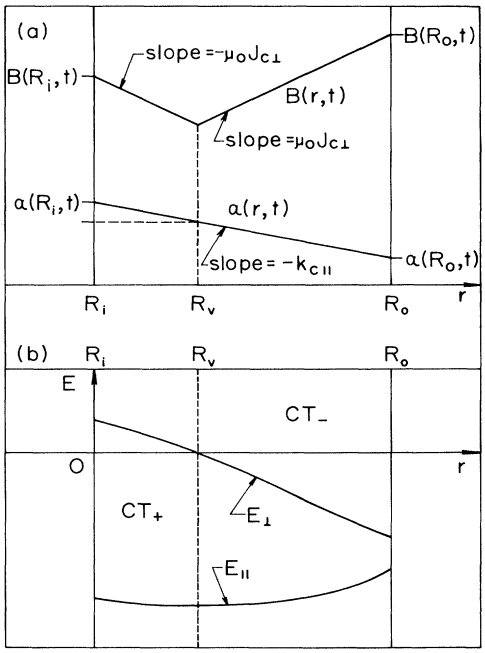

FIG. 4. (a) **B** and (b) **E** behavior inside the cylindrical shell for the flux-line-cutting dominated regime. Flux-line cutting is occurring throughout the entire shell; however, there are two T zones for satisfying the boundary conditions as discussed in Sec. III.

$$B(R_o)-B(R_i)=B(R_o)k_{c\parallel}W\cot\alpha(R_o)<\mu_0 J_{c\perp}W \ .$$

This suggests that the CT zone spanning the wall is divided into a CT_+ (cutting and transport to the right) zone and a CT_- (cutting and transport to the left) zone [see Fig. 4(a)]. The boundary R_v between zones is defined by

$$\frac{W_v}{W}=\frac{1}{2}\left[1-\frac{\tan\gamma_c}{\tan\alpha(R_o)}\right] , \tag{36}$$

where $W_v=R_v-R_i$. Note that when $\alpha(R_o)=\gamma_c$, $W_v=0$, and that when $\alpha(R_o)=\pi/2$, $W_v=W/2$.

In this regime we still have

$$E_\phi(R_i,t)=-\tfrac{1}{2}R\dot{B}_i=-\tfrac{1}{2}R\dot{B}_a \ .$$

In the wall $d\alpha/dr=-k_{c\parallel}$ or $J_\parallel=-J_{c\parallel}$; thus, $E_\parallel<0$. However, for $r>R_v$, we have $dB/dr>0$ and $J_\perp=-J_{c\perp}$, such that $E_\perp<0$. For $r<R_v$, we have $dB/dr<0$ and $J_\perp=+J_{c\perp}$, such that $E_\perp>0$. This implies that $E_\perp=0$ at $r=R_v$. Solving Eqs. (29) and (30) with the above-stated boundary conditions, we obtain [see Fig. 4(b)]

$$E_\parallel(r,t)=\frac{E_\phi}{\sin\alpha(R_v,t)}\cos k_{c\parallel}(r-R_v) \ , \tag{37}$$

$$E_\perp(r,t)=\frac{E_\phi}{\sin\alpha(R_v,t)}\sin k_{c\parallel}(r-R_v) \ . \tag{38}$$

$E_z(t)$ is again independent of r in both the CT_+ and CT_- zones and is given by

$$E_z(t)=E_\phi\cot\alpha(R_v,t) \ . \tag{39}$$

Since we have assumed $k_{c\parallel}W\ll 1$,

$$\alpha(R_v)=\alpha(R_o)+k_{c\parallel}(W-W_v)\cong\alpha(R_o) \ ,$$

we have, to good approximation,

$$E_z(t)=-\tfrac{1}{2}R\dot{B}_a\cot\alpha(R_o)=-\tfrac{1}{2}R\dot{B}_a\frac{B_a}{B_\phi} \tag{40}$$

for $B_\phi/B_a>J_{c\parallel}/J_{c\perp}$.

In both cases, $\tan\alpha(R_o)<\tan\gamma_c$ and $\tan\alpha(R_o)>\tan\gamma_c$,

$$E_\phi=-\tfrac{1}{2}R\dot{B}_i=-\tfrac{1}{2}R\dot{B}_a$$

remains the same; however, E_z changes sign at γ_c. Thus, at γ_c the direction of **E** changes sharply by approximately 90° in a fashion similar to that discussed in Ref. 26.

Note that, for the $\tan\alpha(R_o)>\tan\gamma_c$ regime, $\dot{B}_a>0$ and $\dot{B}_i>0$, i.e., the magnitude of the magnetic field inside the hole is increasing even when there is a transport-outward zone (i.e., flux transport in the positive-r direction) near the inner surface of the cylindrical shell.

The electric-field components at the inner surface obey $E_\perp(R_i,t)>0$ and $E_\parallel(R_i,t)<0$. The condition $E_\perp>0$ indicates that magnetic flux directed along $\hat{\alpha}(R_i,t)$ is being transported from the inner surface in an outward (positive-r) direction. Similarly, $E_\parallel<0$ indicates that magnetic flux directed along $-\hat{\beta}(R_i,t)$ is being transported inward to the inner surface. The ϕ component of **E** is

$$E_\phi(R_i,t)=-(|E_\parallel|\sin\alpha-E_\perp\cos\alpha)$$
$$=-\tfrac{1}{2}R\dot{B}_i\cong-\tfrac{1}{2}R\dot{B}_a \ , \tag{41}$$

as required. Thus, although $E_\perp$ tends to transport the z-directed flux out of the hole, $E_\parallel$ opposes and overcomes this effect. Flux-line-cutting processes tend to transport the z-directed flux into the hole. So long as $|E_\parallel|\sin\alpha>E_\perp\cos\alpha$, we have $\dot{B}_i>0$.

Certainly, *without* flux-line cutting there would be no way for $B(R_i,t)$ at the inner surface to increase when the B profile is like that of Fig. 4(a), because that form of the B profile implies a current density producing an *outward* Lorentz force on any vortices in the region $R_i<r<R_v$.

IV. ac LOSSES

Consider the case in which the applied magnetic field is made up of two bias components $B_o\hat{z}$ and $B_\phi\hat{\phi}$, and an ac component $b_a(t)\hat{z}$ of amplitude $b_o\ll B_o$, such that the axial field is

$$\mathbf{B}_a(t)=\hat{z}[B_o+b_a(t)] \ ,$$

and the net externally applied magnetic field is $\mathbf{B}_s=\mathbf{B}_a(t)+B_\phi\hat{\phi}$ as sketched in Fig. 5. Assume that this field has been cycling for a long time and then the α profiles have the shape shown in Fig. 6.

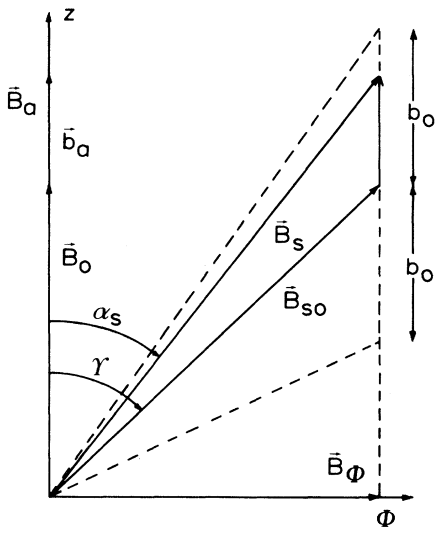

FIG. 5. Sketch of the fields applied parallel to the outer surface. Two dc-bias fields $\mathbf{B}_\phi$ and $\mathbf{B}_0$ are applied in the ϕ and z directions, respectively. In addition, an ac field $\mathbf{b}_a$ of amplitude $b_0\ll B_0$ is applied parallel to the z direction. To lowest order in b_0, the magnitude $B_s=B_{s0}+b_a\cos\gamma$ of the net applied field oscillates between $B_s=B_{s0}\pm b_0\cos\gamma$, and the angle $\alpha_s=\gamma-(b_a/B_{s0})\sin\gamma$ between the net applied field and the z direction oscillates between $\alpha_s=\gamma\mp(b_0/B_{s0})\sin\gamma$. B_{s0} and γ are the magnitude and direction, respectively, of the external **B** field when no external ac component is applied.

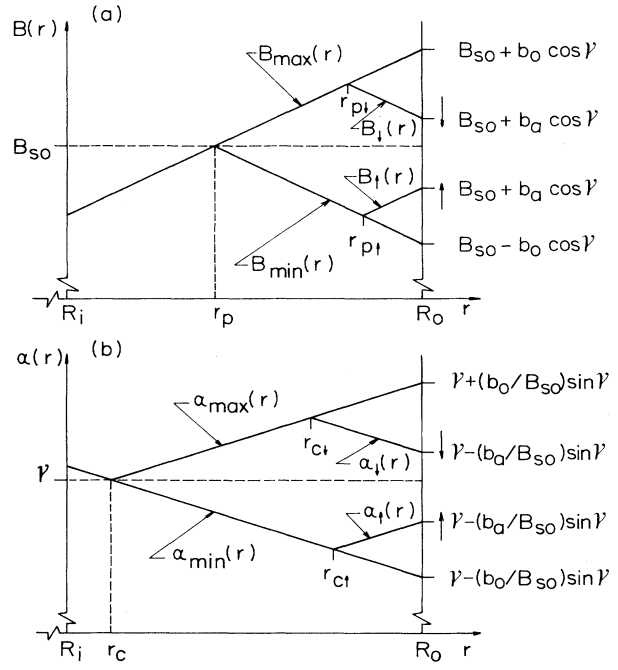

FIG. 6. Sketch of (a) extremal field magnitude profiles B_{max} and B_{min} and the B_s-increasing and B_s-decreasing profiles $B_\uparrow$ and $B_\downarrow$ vs r, as calculated from $|\partial B/\partial r|=\mu_0 J_{c\perp}$ for partial penetration of the changing B profile; (b) extremal field-angle profiles α_{max} and α_{min} and the α_s-increasing and α_s-decreasing profiles $\alpha_\uparrow$ and $\alpha_\downarrow$, vs r, calculated from $|\partial\alpha/\partial r|=k_{c\parallel}$ for partial penetration of the changing α profile.

The magnitude and direction of the net external **B** field are

$$B_s=B_{s0}+b_a\cos\gamma \tag{42}$$

and

$$\alpha_s=\gamma-(b_a/B_{s0})\sin\gamma\ , \tag{43}$$

respectively, where $B_{s0}=(B_0^2+B_\phi^2)^{1/2}$ and $\gamma=\arctan(B_\phi/B_0)$ are the magnitude and direction of the external **B** field when no ac component is applied.

The ac loss per unit area of the shell per cycle W_a can be calculated integrating the Poynting vector over one cycle

$$W_a'=-\mu_0^{-1}\oint dt\,\hat{\mathbf{r}}\cdot\mathbf{E}(R_o,t)\times\mathbf{B}_s(t)\ . \tag{44}$$

We can write

$$\begin{aligned}\mathbf{r}\cdot\mathbf{E}(R_o,t)\times\mathbf{B}_s(t)&=\mathbf{r}\times\mathbf{E}(R_o,t)\cdot\mathbf{B}_s(t)\\&=-E_z(R_o,t)B_\phi(R_o,t)\\&\quad+E_\phi(R_o,t)B_z(R_o,t)\ ,\end{aligned} \tag{45}$$

and from Faraday's law we obtain

$$E_z(R_o,t)=E_{z0}+\frac{\partial}{\partial t}\int_0^{R_o}B_\phi dr \tag{46}$$

and

$$E_\phi(R_o,t)=-\frac{1}{R_o}\int_0^{R_o}r\frac{\partial B_z}{\partial t}dr\ . \tag{47}$$

Since B_ϕ is independent of time, E_z is independent of r, consequently, the time integral of E_zB_ϕ over one entire cycle is zero.

Two regimes must be considered: (a) the changing B and α profiles do not penetrate though the entire shell thickness, in such a case the **B** field in the hole does not change, and (b) the changing B and α profiles do penetrate all the way through the shell and the **B** field in the hole changes producing a large ϕ component of the electric field.

Figure 6 shows the B and α profiles for the first regime, they are linear to lowest order in b_a, their extrema are

$$B_{max}(r)=B_{s0}+b_0\cos\gamma-\mu_0J_{c\perp}(R_o-r)\ , \tag{48a}$$

$$B_{min}(r)=B_{s0}-b_0\cos\gamma+\mu_0J_{c\perp}(R_o-r)\ , \tag{48b}$$

$$\alpha_{max}(r)=\gamma-(b_0/B_{s0})\sin\gamma-k_{c\parallel}(R_o-r)\ , \tag{49a}$$

and

$$\alpha_{min}(r)=\gamma+(b_0/B_{s0})\sin\gamma+k_{c\parallel}(R_o-r)\ , \tag{49b}$$

and the depths within which B and α change during one cycle are

$$r_p=R_o-(b_0/\mu_0J_{c\perp})\cos\gamma \tag{50}$$

and

$$r_c=R_o-(b_0/\mu_0J_{c\parallel})\sin\gamma\ , \tag{51}$$

respectively. Depending upon the values of $J_{c\perp}$, $J_{c\parallel}$, and γ, r_p can be larger than, equal to, or smaller than r_c; Fig. 6 shows the case in which $r_p>r_c$.

During the b_a-decreasing half-cycle, which corresponds to increasing α, the ϕ component of the electric field at the outer surface is given by

$$\begin{aligned}E_{\phi\downarrow}(R_o)&=-\frac{1}{R_o}\left[\int_{r_{c\uparrow}}^{r_{p\downarrow}}r\,dr\frac{d}{dt}[B_{max}(r)\cos\alpha_\uparrow(r,t)]+\int_{r_{p\downarrow}}^{R_o}r\,dr\frac{d}{dt}[B_\downarrow(r,t)\cos\alpha_\uparrow(r,t)]\right]\\&=-\frac{1}{2}\left[\left[R_o-\frac{r_{c\uparrow}^2}{R_o}\right]\sin^2\gamma+\left[R_o-\frac{r_{p\downarrow}^2}{R_o}\right]\cos^2\gamma\right]\dot{b}_a\\&=-\frac{\dot{b}_a}{2\mu_0}\left[(b_0-b_a)\left[\frac{\sin^3\gamma}{J_{c\parallel}}+\frac{\cos^3\gamma}{J_{c\perp}}\right]-\frac{(b_0-b_a)^2}{4\mu_0R_o}\left[\frac{\sin^4\gamma}{J_{c\parallel}^2}+\frac{\cos^4\gamma}{J_{c\perp}^2}\right]\right]\ ,\end{aligned} \tag{52}$$

where we have used

$$r_{c\uparrow}=R_o-\frac{b_0-b_a}{2\mu_0 J_{c\parallel}}\sin\gamma \tag{53}$$

and

$$r_{p\downarrow}=R_o-\frac{b_0-b_a}{2\mu_0 J_{c\perp}}\cos\gamma\ . \tag{54}$$

Similarly,

$$E_{\phi\uparrow}(R_o)=-\frac{\dot{b}_a}{2\mu_0}\left[(b_0+b_a)\left[\frac{\sin^3\gamma}{J_{c\parallel}}+\frac{\cos^3\gamma}{J_{c\perp}}\right]-\frac{(b_0+b_a)^2}{4\mu_0 R_o}\left[\frac{\sin^4\gamma}{J_{c\parallel}^2}+\frac{\cos^4\gamma}{J_{c\perp}^2}\right]\right]. \tag{55}$$

The resulting loss per unit area of the outer surface is, from Eq. (44),

$$W_a'=\frac{2b_0^3}{3\mu_0^2}\left[\frac{\sin^3\gamma}{J_{c\parallel}}+\frac{\cos^3\gamma}{J_{c\perp}}\right]. \tag{56}$$

In this expression, which is valid to order b_0^3, we have neglected higher-order terms which are smaller than the terms retained by factors of $b_0/\mu_0 R_o J_{c\parallel}$ or $b_0/\mu_0 R_o J_{c\perp}$.

Equation (56) was derived in Ref. 4 and gives the loss per unit area per cycle for a semi-infinite superconductor, or the loss per unit area per cycle at each surface of a superconducting slab whose thickness is more than twice the largest of the depths within which B and α change during one cycle. The result is also valid for $r_p<r_c$.

For calculating the loss expression corresponding to the regime in which the changing profiles sweeps across the entire shell thickness, we define the quantities

$$b_c=\mu_0 J_{c\parallel}W/\sin\gamma \tag{57}$$

and

$$b_p=\mu_0 J_{c\perp}W/\cos\gamma\ . \tag{58}$$

Their sizes, relative to b_0, determine the degree of penetration of the changing profiles. b_c is the value of b_0 when $R_o-r_c=W$ and b_p is the value of b_0 when $R_o-r_p=W$.

Again, b_c can be larger than, equal to, or smaller than b_p, depending upon $J_{c\parallel}$, $J_{c\perp}$, and γ. The ac loss per cycle per unit area of the outer surface when $b_p<b_c$ and $b_0>b_p$ is, to leading order,

$$W_a'=\frac{2R_o W J_{c\perp}(b_0-b_p)}{\cos\gamma}\ . \tag{59}$$

This regime corresponds to $\tan\gamma<\tan\gamma_c$ and the behavior is flux-transport dominated [see Fig. 3(a)] in the sense that during the lossiest part of the cycle

$$B(R_i)=B(R_o)\pm\mu_0 J_{c\perp}W\ . \tag{60}$$

The regime in which $\tan\gamma>\tan\gamma_c$ is flux-line-cutting dominated [see Fig. 4(a)], in the sense that, during the lossiest part of the cycle,

$$\alpha(R_i)=\alpha(R_o)\pm\mu_0 J_{c\parallel}W\ . \tag{61}$$

In this regime the ac loss per cycle per unit area of the outer surface of the cylinder when $b_0>b_c$ is, to leading order,

$$W_a'=\frac{2R_o W J_{c\parallel}(b_0-b_c)}{\sin\gamma}\ . \tag{62}$$

In the ac-loss expressions (59) and (62) we have neglected terms smaller by a factor $W/R_o\ll 1$ than those shown. Thus, although the retained terms dominate for sufficiently large values of (b_0-b_p) or (b_0-b_c), they become comparable with the neglected terms when $(b_0-b_p)\le b_p(W/R_o)$ or $(b_0-b_c)\le b_c(W/R_o)$. The complete expressions for the ac losses, which are too complicated to present here, reduce to Eq. (56) in the limit $b_0\to b_p$ or $b_0\to b_c$.

Equations (59) and (62) are proportional to R_o; thus, they do not reduce to those of slab geometry when $R_o\gg W$. The reason for this behavior is that, while a finite slab is subjected to the same changing **B** field on both sides, the cylindrical shell is not. For the finite slab,[4] **B** is symmetric with respect to the slab midpoint x_m and $\mathbf{E}(x_m,t)=0$. For the cylindrical shell, **B** is not symmetric with respect to the shell half-thickness, nor is $\mathbf{E}=0$ there; as shown in Eqs. (40) and (41), for example, E_z is a constant independent of r and E_ϕ increases in magnitude as the radius of the shell increases.

V. SUMMARY AND DISCUSSION

A brief discussion of the general critical-state model was presented in Sec. II. In Sec. III we showed how a very thin cylindrical shell must be treated when the external B field is changing direction and magnitude. We wrote down the assumptions one must make in order to treat the cylindrical shell as a slab. In the case the B and α profiles are changing over the entire shell (full penetration), two regimes arise: flux-pinning dominated and flux-line-cutting dominated. We calculated the electromagnetic response under both regimes. An apparent paradox shows up in the latter regime when $E_\perp$-transported magnetic flux travels outward from the hole, while the magnitude of the **B** field inside the hole is increasing. It was demonstrated that $E_\parallel$-transported magnetic flux overcomes this and that the net trend is the mentioned increasing in B inside the hole. Without the flux-line-cutting contribution there is no way of solving this paradox.

In Sec. IV we calculated the losses when the axial external **B** field had an ac component. Even when the cylindrical shell can be taken as a slab when its radius is large compared to its thickness, great care must be taken when establishing the boundary conditions. Two cases must be considered: partial penetration of the changing B and α profiles, and full penetration of them. For partial penetration in the cylindrical shell, the **B** and **E** fields behave similarly to the way they do in slab geometry. However, when full penetration occurs, the behavior of

those fields within the shell differs dramatically from their behavior in the slab, it is in this regime of full penetration when $E_\phi = -\frac{1}{2}R\dot{B}_i$ for the cylindrical shell.

For the slab, one considers that the magnetic field is exactly the same on both surfaces. The electric and magnetic fields inside the slab are then symmetric with respect to the midplane and, in particular, $\mathbf{E}=0$ at that point. In the cylindrical shell the magnetic-field components at the inner surface are generally different from those on the outer surface. In this paper we considered the case for which a thin cylindrical shell carries no net longitudinal current, which, by Ampère's law, means that the azimuthal components of the magnetic fields are nearly the same at the inner and outer surfaces. On the other hand, while the axial field component at the outer surface is determined by the longitudinal applied field, the axial field component at the inner surface depends upon the magnitude and sign of the azimuthal induced supercurrents. When an increasing longitudinal field is applied, the axial magnetic field inside the shell may be smaller than that outside, but can increase whenever longitudinal flux leaks in through the wall. (Similarly, when the applied longitudinal field decreases, the axial magnetic field inside the shell may be larger than that outside, but can decrease whenever longitudinal flux leaks out.) The line integral of the electric field around the circumference is proportional to the time rate of change of the longitudinal flux through the hole, and as a consequence the losses contain a term proportional to the radius R_o. These loss expressions cannot, in any way, reduce to the loss expressions in slab geometry.

ACKNOWLEDGMENTS

Ames Laboratory is operated for the U.S. Department of Energy by Iowa State University under Contract No. W-7405-Eng-82. This work was supported in part by the Director for Energy Research, Office of Basic Energy Sciences.

---

*Present address: Department of Physics, McMaster University, Hamilton, Ontario, Canada L85 4M1.

[1]J. R. Clem, Phys. Rev. B **26**, 2463 (1982).
[2]J. R. Clem and A. Pérez-González, Phys. Rev. B **30**, 5041 (1984).
[3]A. Pérez-González and J. R. Clem, Phys. Rev. B **31**, 7048 (1985).
[4]A. Pérez-González and J. R. Clem, Phys. Rev. B **32**, 2909 (1985).
[5]A. Pérez-González and J. R. Clem, J. Appl. Phys. **58**, 4326 (1985).
[6]J. R. Cave, J. E. Evetts, and A. M. Campbell, J. Phys. (Paris) Colloq. **39**, C6-614 (1978).
[7]M. A. R. LeBlanc and B. R. Kiggins, Solid State Commun. **8**, 633 (1970).
[8]J. P. Lorrain, M. A. R. LeBlanc, and A. Lachaine, Can. J. Phys. **57**, 1458 (1979).
[9]R. Boyer, Ph.D. thesis, University of Ottawa, Canada, 1977.
[10]R. Boyer, G. Fillion, and M. A. R. LeBlanc, J. Appl. Phys. **51**, 1692 (1980).
[11]R. Boyer and M. A. R. LeBlanc, Solid State Commun. **24**, 261 (1977).
[12]J. R. Cave and M. A. R. LeBlanc, J. Appl. Phys. **53**, 1631 (1982).
[13]G. Fillion, R. Gauthier, and M. A. R. LeBlanc, Phys. Rev. Lett. **43**, 86 (1979).
[14]R. Gauthier, Ph.D. thesis, University of Ottawa, Canada, 1976.
[15]R. Gauthier and M. A. R. LeBlanc, IEEE Trans. Magn. **MAG-13**, 560 (1977).
[16]A. Lachaine, Ph.D. thesis, University of Ottawa, Canada, 1976.
[17]A. Lachaine and M. A. R. LeBlanc, in *Low Temperature Physics LT-13,* edited by K. D. Timmerhaus, W. J. O'Sullivan, and E. F. Hammel (Plenum, New York, 1974), Vol. 3, p. 247.
[18]A. Lachaine and M. A. R. LeBlanc, IEEE Trans. Magn. **MAG-11**, 336 (1975).
[19]A. Lachaine, M. A. R. LeBlanc, and J. P. Lorrain, Physica **107B**, 433 (1981).
[20]M. A. R. LeBlanc and B. C. Belanger, Appl. Phys. Lett. **8**, 291 (1966).
[21]H. London, Phys. Lett. **6**, 162 (1963).
[22]C. P. Bean, Rev. Mod. Phys. **36**, 31 (1964).
[23]A. M. Campbell and J. E. Evetts, Adv. Phys. **21**, 199 (1972).
[24]D. G. Walmsley, J. Phys. F **2**, 510 (1972).
[25]A. G. Saif, Phys. Status Solidi B **149**, 657 (1988).
[26]J. R. Clem and A. Pérez-González, Phys. Rev. B **33**, 1601 (1986).